Acta Crystallographica Section F
Structural Biology and Crystallization Communications
ISSN 1744-3091

Purification and crystallization of the catalytic PRONE domain of RopGEF8 and its complex with Rop4 from *Arabidopsis thaliana*

Christoph Thomas, Michael Weyand, Alfred Wittinghofer and Antje Berken*

Department of Structural Biology, Max Planck Institute of Molecular Physiology, Otto-Hahn-Strasse 11, 44227 Dortmund, Germany

Correspondence e-mail: antje.berken@mpi-dortmund.mpg.de

Received 11 May 2006
Accepted 19 May 2006

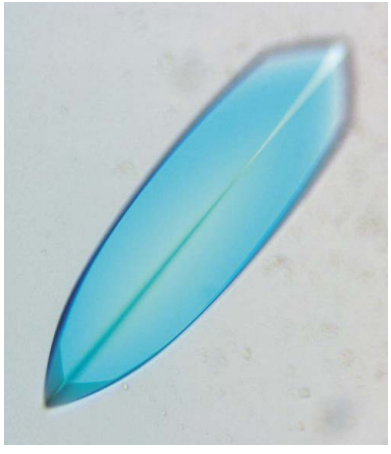

The PRONE domain of the guanine nucleotide exchange factor RopGEF8 (PRONE8) was purified and crystallized free and in complex with the Rho-family protein Rop4 using the hanging-drop vapour-diffusion method. PRONE8 crystals were obtained using NaCl as precipitating agent and belong to the hexagonal space group $P6_522$. Native and anomalous data sets were collected using synchrotron radiation at 100 K to 2.2 and 2.8 Å resolution, respectively. Crystals of the Rop4–PRONE8 complex belonging to space group $P6_3$ were obtained using Tacsimate and PEG 3350 as precipitating agents and diffracted to 3.1 Å resolution.

1. Introduction

Small guanine nucleotide binding proteins (G proteins) belonging to the Rho family called Rops (Rho of plants) play a vital role as regulators of signal transduction in plants (for reviews, see Zheng & Yang, 2000; Yang, 2002; Gu *et al.*, 2004). Rops participate in pathways that influence growth and development and the adaptation of plants to various environmental situations. As members of the Ras superfamily, Rops function as molecular switches that are turned on by exchanging bound GDP for GTP. Reaction cascades are then induced *via* effector molecules to generate a cellular response until GTP hydrolysis returns the switch back to the inactive state. The activation status of the switch is strictly regulated by GTPase activating proteins (RopGAPs), which accelerate the slow intrinsic GTPase activity of Rop (Wu *et al.*, 2000), and by novel guanine nucleotide exchange factors (RopGEFs) that catalyze the dissociation of the tightly bound nucleotide (Berken *et al.*, 2005; Gu *et al.*, 2006). The higher concentration of GTP *versus* GDP in the cell drives the exchange reaction towards the production of the GTP-bound state, resulting in the activation of Rop signalling *in vivo*.

The plant-specific RopGEFs represent a unique family of exchange factors that display no homology to any known RhoGEFs from animals and fungi. They comprise a highly conserved catalytic domain termed PRONE (plant-specific Rop nucleotide exchanger) with exclusive substrate specificity for members of the Rop family (Berken *et al.*, 2005). *Arabidopsis thaliana* contains 11 Rops (reviewed in Yang, 2002) and 14 RopGEFs that are expressed in various tissues (Kaothien *et al.*, 2005; Gu *et al.*, 2006). The PRONE domain of RopGEF1 was shown to be necessary and sufficient to promote nucleotide release from Rop4 with catalytic properties comparable to RhoGEFs of the diffuse B-cell lymphoma (Dbl) type known from animals and fungi (Berken *et al.*, 2005). However, the molecular mechanism of RopGEF catalysis remains elusive.

The Dbl-type GEFs from animals and fungi have been characterized in more detail. They comprise a tandem arrangement of a Dbl-homology (DH) and a pleckstrin-homology (PH) domain and several structures of the DH or the DH/PH module have been solved either free or in complex with the respective Rho substrate (reviewed in Zheng, 2001; Erickson & Cerione, 2004; Rossman *et al.*, 2005). These structures reveal that the catalytic DH domain is an all-helical unit which interacts intensively with the two switch regions of the Rho proteins, resulting in their displacement and remodelling, while the rest of the molecule remains essentially unperturbed in the complexes. These structural changes interfere with magnesium

binding and the phosphate moiety of the nucleotide and thus promote nucleotide release. A similar mechanism applies to the RhoGEF SopE from *Salmonella typhimurium*, although this protein is structurally unrelated to Dbl-type GEFs (Buchwald *et al.*, 2002), and it has been proposed that a so-called 'push-and-pull mechanism' involving the switch regions is a common mechanistic principle of GEF action (Vetter & Wittinghofer, 2001).

In order to gain insight into the molecular mechanisms that underlie PRONE-mediated RopGEF catalysis, we crystallized the PRONE domain of the pollen-expressed RopGEF8 from *A. thaliana* alone and in complex with Rop4.

2. Experimental

2.1. Overexpression and purification

Constructs for the PRONE domain of RopGEF8 comprising residues 76–440 (PRONE8; 41.5 kDa) and for Rop4 (residues 1–180; 19.8 kDa) lacking the C-terminal prenylation motif were generated by PCR and cloned in pGEX-6P-1 and pGEX-4T-1 vectors (Amersham Biosciences), respectively. Protein expression in *Escherichia coli* BL21-CodonPlus(DE3)-RIL (Stratagene) using Terrific Broth (TB) was induced at an optical density (OD_{600}) of 0.6 with 0.3 m*M* isopropyl β-D-thiogalactopyranoside and the culture was further grown overnight at 293 K and 180 rev min^{-1}. For selenomethionine (SeMet) labelling, PRONE8 was expressed under the same conditions in a methionine-biosynthesis inhibiting minimal medium without methionine containing 50 mg l^{-1} L-selenomethionine (Van Duyne *et al.*, 1993). Harvested cells were resuspended in buffer (30 m*M* HEPES pH 7.5, 100 m*M* NaCl, 5 m*M* DTE or 20 m*M* DTE for SeMet-substituted PRONE8 and additionally 5 m*M* $MgCl_2$ in the case of Rop4) including 0.5%(*v*/*v*) Triton X-100 and 1 m*M* phenylmethylsulfonylfluoride. The suspension was subjected to sonication and the soluble cell extract after ultracentrifugation (60 min, 95 000*g*, 277 K) was applied onto an equilibrated glutathione Sepharose column. The column was washed until the baseline was reached again and the glutathione-*S*-transferase tag was removed by on-column digestion at 277 K overnight with 10 mg PreScission protease (Amersham Biosciences) or 500 U thrombin (Serva). Cleaved proteins were eluted, subjected to gel filtration using the same buffer as before on a Superdex 75 column (Amersham Biosciences) for Rop4 or a Superdex 200 column (Amersham Biosciences) for PRONE8 and finally concentrated by ultrafiltration (Amicon, Millipore). Cleaved Rop4 contained an additional glycine and serine residue at the amino-terminus as a result of the cloning procedure. For the same reason, PRONE8 contained additional amino acids (Gly, Pro, Leu, Gly, Ser) at the N-terminus.

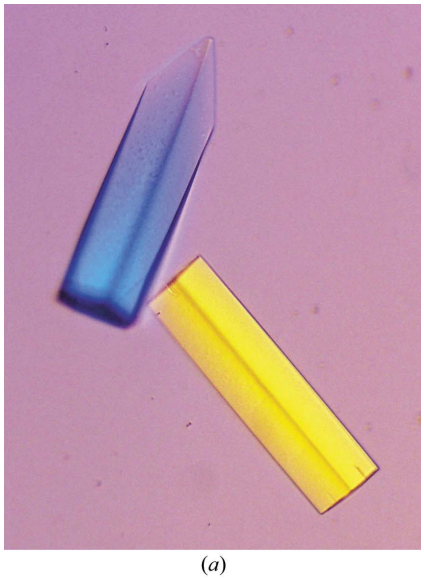

(*a*)

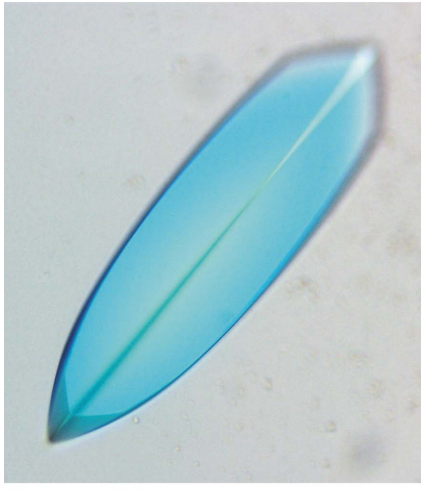

(*b*)

Figure 1
Photographs of (*a*) native PRONE8 crystals (approximate dimensions 0.6 × 0.15 × 0.15 mm) and (*b*) a crystal of the SeMet derivative (approximate dimensions 0.7 × 0.2 × 0.2 mm).

2.2. Crystallization

Native and SeMet-substituted PRONE8 and its complex with Rop4 were crystallized using the hanging-drop vapour-diffusion technique. Initial conditions for the crystallization of PRONE8 were determined with Crystal Screen 2 (Hampton Research) and were optimized to the following conditions: 1 µl of a 5 mg ml^{-1} (native) or an 8 mg ml^{-1} (SeMet derivative) protein solution was mixed with 1 µl reservoir solution [740 m*M* NaCl and 100 m*M* sodium citrate pH 5.6 (native PRONE8) or 700 m*M* NaCl and 100 m*M* sodium citrate pH 5.5 (SeMet derivative)]. The reservoir volume was 1 ml. PRONE8 crystallized overnight at 296 K. Native PRONE8 crystals reached final dimensions of 0.6 × 0.15 × 0.15 mm (Fig. 1*a*); crystals of the SeMet derivative reached dimensions of 0.7 × 0.2 × 0.2 mm. In addition to the hexagonal crystal form that was observed for the native protein, the SeMet derivative formed crystals in the same crystallization drop that were also hexagonal, but tapered off at the

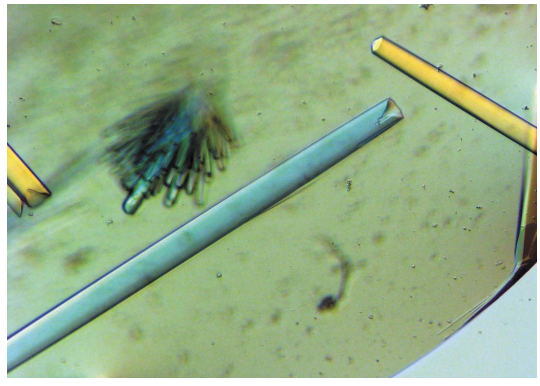

Figure 2
Photograph of Rop4–PRONE8 crystals (approximate dimensions 0.9 × 0.05 × 0.05 mm).

ends (Fig. 1*b*). Crystals were collected, cryoprotected in 100 m*M* sodium citrate pH 5.5 (SeMet derivative) or pH 5.6 (native), 30 m*M* HEPES pH 7.5, 800 m*M* NaCl and 20%(*v*/*v*) glycerol and frozen in liquid nitrogen. For crystallization of the Rop4–PRONE8 complex, both purified proteins were mixed in an equimolar ratio and incubated for 30 min at room temperature without adding further components. This mixture was used for crystallization. Initial conditions were determined with the Index Screen (Hampton Research) and further optimized to the following conditions. Crystals appeared at 293 K after 2 d in hanging drops consisting of 2 µl protein solution (18 mg ml^{-1} of the preformed complex, see above) and 1 µl reservoir [18%(*v*/*v*) Tacsimate (Hampton Research), 4%(*w*/*v*) PEG 3350, 0.1 *M* Tris–HCl pH 7.3]. The reservoir volume was 1 ml. Crystals reached final dimensions of 0.9 × 0.05 × 0.05 mm (Fig. 2) and were frozen in liquid nitrogen using the reservoir solution containing 20%(*v*/*v*) glycerol as cryoprotectant. The presence of both proteins in the Rop4–PRONE8 crystals was verified by SDS–PAGE (Laemmli, 1970) (Fig. 3). For this purpose, the crystals were washed four times with reservoir solution and subsequently dissolved in 30 m*M* HEPES pH 7.5 and 100 m*M* NaCl.

2.3. Data collection

All data sets were collected at the Swiss Light Source (Villigen, Switzerland) at 100 K using a MAR 225 CCD detector. In order to solve the phase problem, a data set from SeMet-substituted PRONE8 was collected at beamline X10SA (PXII) at a wavelength of 0.9793 Å. SeMet incorporation was proven by a fluorescence scan, which led to a clear absorption peak at the absorption edge of selenium. The crystal-to-detector distance for data collection was 330 mm, the oscillation width per frame was 0.25° and 450 frames were collected. The best diffracting crystal later turned out to be one grown from the SeMet derivative. A native data set of this crystal was collected on the same beamline at a wavelength of 0.8985 Å (crystal-to-detector distance, 300 mm; oscillation width per frame, 0.5°; 280 frames collected). Two native data sets were collected from one Rop4–PRONE8 crystal on beamline X06SA (PXI) at a wavelength of 0.9788 Å (crystal-to-detector distance, 290 or 310 mm; oscillation width per frame, 1 or 0.5°; 80 or 160 frames collected) and were merged. Data-collection statistics are shown in Table 1.

Data were indexed, integrated and scaled with the *XDS* package (Kabsch, 1993). Crystals of PRONE8 belong to space group $P6_522$ and crystals of Rop4–PRONE8 to space group $P6_3$.

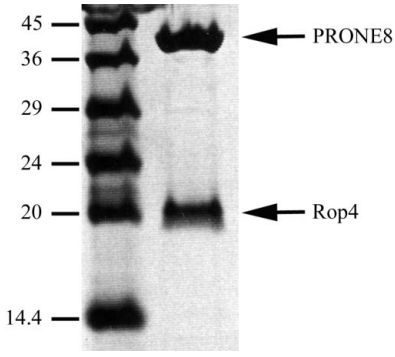

Figure 3
SDS–PAGE (14%; Coomassie blue staining) of dissolved Rop4–PRONE8 crystals (left lane, molecular-weight standards in kDa; right lane, sample of the dissolved crystals).

Table 1
Data-collection statistics.

Values in parentheses are for the highest resolution shell.

	Native data set (PRONE8)	SeMet-PRONE8	Rop4–PRONE8
Wavelength (Å)	0.8985	0.9793	0.9788
Resolution (Å)	20–2.2 (2.3–2.2)	20–2.8 (2.9–2.8)	50–3.1 (3.2–3.1)
Space group	$P6_522$	$P6_522$	$P6_3$
Unit-cell parameters (Å)	$a = b = 114.3$, $c = 319.0$	$a = b = 111.9$, $c = 317.5$	$a = b = 211.2$, $c = 81.1$
V_M (Å^3 Da^{-1})	3.6	3.5	4.3
Total measurements	884737	366548	314533
Unique reflections	62938	54359	37649
Average redundancy	14.1 (6.7)	6.7 (4.4)	8.4 (5.1)
$I/\sigma(I)$	21.0 (4.2)	17.3 (3.7)	16.8 (4.2)
Completeness (%)	99.2 (95.9)	99.3 (97.6)	99.7 (99.8)
Wilson *B* factor (Å^2)	42	61	57
R_{sym}†	8.5 (45.2)	7.6 (39.6)	16.0 (43.9)

† $R_{sym} = \sum |I(h)_j - \langle I(h)\rangle| / \sum I(h)_j$, where $I(h)_j$ is the scaled observed intensity of the *j*th symmetry-related observation of reflection *h* and $\langle I(h)_j\rangle$ is the mean value.

3. Results and discussion

Here we describe the overexpression, purification and crystallization of the catalytic PRONE domain of RopGEF8 from *A. thaliana*. The protein was overexpressed in *E. coli* as a native protein or an SeMet derivative and purified by affinity chromatography. These procedures yielded 8 mg pure protein per litre of expression culture, leading to protein crystals useful for X-ray data collection with statistics given in Table 1. Crystals diffracted to 2.2 Å (native) or 2.8 Å (SeMet derivative) resolution. The asymmetric unit of the PRONE8 crystals is estimated to contain two PRONE8 molecules, corresponding to a V_M of 3.6 Å^3 Da^{-1} (Matthews, 1968) and a solvent content of 65.8%. The Rop4–PRONE8 complex could be formed by simply mixing PRONE8 with purified Rop4 protein, resulting in crystals that diffracted to 3.1 Å. The Rop4–PRONE8 crystals are estimated to contain two heterodimers per asymmetric unit, with a V_M of 4.3 Å^3 Da^{-1} and a solvent content of 70.9%. Searching for the selenium sites, we could localize 27 out of 28 possible sites, corresponding to the two PRONE8 molecules in the asymmetric unit of the SeMet–PRONE8 crystals. We are currently refining the selenium sites for the structure determination of PRONE8, which will subsequently be used as a search model for molecular replacement to determine the structure of the Rop4–PRONE8 complex.

The authors are grateful to the staff of the SLS, Villigen, Switzerland for technical support and Eckhard Hofmann, Nils Schrader, Ilme Schlichting, Anton Meinhart and Wulf Blankenfeldt for data collection. CT is supported by the Boehringer Ingelheim Fonds; AB thanks the Deutsche Forschungsgemeinschaft (Priority Program SSP1150) for support.

References

Berken, A., Thomas, C. & Wittinghofer, A. (2005). *Nature (London)*, **436**, 1176–1180.
Buchwald, G., Friebel, A., Galán, J. E., Hardt, W. D., Wittinghofer, A. & Scheffzek, K. (2002). *EMBO J.* **21**, 3286–3295.
Erickson, J. W. & Cerione, R. A. (2004). *Biochemistry*, **43**, 837–842.
Gu, Y., Li, S., Lord, E. M. & Yang, Z. (2006). *Plant Cell*, **18**, 366–381.
Gu, Y., Wang, Z. & Yang, Z. (2004). *Curr. Opin. Plant Biol.* **7**, 527–536.
Kabsch, W. (1993). *J. Appl. Cryst.* **26**, 795–800.
Kaothien, P., Ok, S. H., Shuai, B., Wengier, D., Cotter, R., Kelley, D., Kiriakopolos, S., Muschietti, J. & McCormick, S. (2005). *Plant J.* **42**, 492–503.
Laemmli, U. K. (1970). *Nature (London)*, **227**, 680–685.

Matthews, B. W. (1968). *J. Mol. Biol.* **33**, 491–497.
Rossman, K. L., Der, C. J. & Sondek, J. (2005). *Nature Rev. Mol. Cell Biol.* **6**, 167–179.
Van Duyne, G. D., Standaert, R. F., Karplus, P. A., Schreiber, S. L. & Clardy, J. (1993). *J. Mol. Biol.* **229**, 105–124.
Vetter, I. R. & Wittinghofer, A. (2001). *Science*, **294**, 1299–1304.
Wu, G., Li, H. & Yang, Z. (2000). *Plant Physiol.* **124**, 1625–1635.
Yang, Z. (2002). *Plant Cell*, **14**, S375-S388.
Zheng, Y. (2001). *Trends Biochem. Sci.* **26**, 724–732.
Zheng, Z. L. & Yang, Z. (2000). *Plant Mol. Biol.* **44**, 1–9.